Transport in Porous Media (2021) 139:381–396
https://doi.org/10.1007/s11242-021-01670-7

Spontaneous Imbibition and Drainage of Water in a Thin Porous Layer: Experiments and Modeling

Luwen Zhuang[1,2] · S. Majid Hassanizadeh[2,5] · Divesh Bhatt[3] · C. J. van Duijn[2,4]

Received: 15 February 2021 / Accepted: 9 August 2021 / Published online: 19 August 2021

Abstract

The typical characteristic of a thin porous layer is that its thickness is much smaller than its in-plane dimensions. This often leads to physical behaviors that are different from three-dimensional porous media. The classical Richards equation is insufficient to simulate many flow conditions in thin porous media. Here, we have provided an alternative approach by accounting for the dynamic capillarity effect. In this study, we have presented a set of one-dimensional in-plane imbibition and subsequent drainage experiments in a thin fibrous layer. The X-ray transmission method was used to measure saturation distributions along the fibrous sample. We simulated the experimental results using Richards equation either with classical capillary equation or with a so-called dynamic capillarity term. We have found that the standard Richards equation was not able to simulate the experimental results, and the dynamic capillarity effect should be taken into account in order to model the spontaneous imbibition. The experimental data presented here may also be used by other researchers to validate their models.

Article Highlights

- **We have presented a set of one-dimensional in-plane imbibition and subsequent drainage experiments in a thin fibrous layer.**
- **The experimental data were simulated using the Richards equation either with classical capillary equation or with a so-call dynamic capillarity term.**
- **The dynamic capillarity effect should be taken into account in order to model the spontaneous imbibition.**

✉ Luwen Zhuang
zhuanglw3@mail.sysu.edu.cn

[1] School of Civil Engineering, Sun Yat-Sen University, Zhuhai 519082, China

[2] Department of Earth Sciences, Utrecht University, P.O. Box 80021, 3508 TA Utrecht, Netherlands

[3] Global Research and Engineering, Kimberly-Clark Corporation, Roswell, GA, USA

[4] Department of Mechanical Engineering, Eindhoven University of Technology, P.O. Box 513, 5600 MB Eindhoven, Netherlands

[5] Stuttgart Center for Simulation Science (SIMTECH), Integrated Research Training Group SFB 1313, Stuttgart University, Stuttgart, Germany

Keywords Dynamic capillarity · In plane · Thin porous layer · Thin porous media · Unsaturated flow

1 Introduction

Thin porous media have attracted much attention because of their importance in various industries. Examples of thin porous media encountered in daily life are hygiene products, paper, filters, fuel cells, membranes, textiles, skin, blood vessel walls, and other biological or manufactured thin materials. A typical characteristic of a thin porous layer is that its thickness is much smaller than its in-plane dimensions. This often leads to physical behaviors different from three-dimensional porous media (e.g., soils). Knowledge of physical phenomena particular to thin porous media is essential for understanding many practical issues (Prat and Agaësse 2015). Among these, unsaturated flow in thin fibrous materials has been encountered in a wide range of applications, such as liquid absorption in paper towels and in hygiene products.

During the past decade, there have been only few experimental and numerical studies of unsaturated flow regimes specific to thin fibrous porous layers (e.g., Landeryou et al. 2005; Reza and Pillai 2010; Aslannejad et al. 2017; Tavangarrad et al. 2018). Landeryou et al. (2005) performed a series of in-plane liquid infiltration experiments on a horizontal or inclined fibrous sheet. The experiments were simulated using both Washburn equation (1921) and Richards equation (1931). The observations could be satisfactorily simulated only when the relationship between relative permeability and liquid saturation in the Richards equation was modified by including a percolation threshold. Ashari and Tafreshi (2009) investigated fluid release in the through-plane direction in thin porous media numerically, using Richards equation. They reconstructed the relationships between relative permeability, capillary pressure, and liquid saturation for primary drainage using a morphological method. Later on, Ashari et al. (2010, 2011) had to use different p_c–S curves in simulations to model fluid flow for a stack of thin layers. The Richards equation was employed to simulate the through-plane drainage experiments. The numerical results could not match the observations without special modifications of boundary conditions. Melciu and Pascovici (2016) modeled the in-plane imbibition in a thin fibrous layer. Both the Washburn equation and single-phase Darcy's law were used to simulate the temporal changes of wetting length. The results obtained using the Washburn equation showed large discrepancy with the observations, whereas the single-phase Darcy's law gave good agreement. Tavangarrad et al. (2018) performed a series of liquid redistribution experiments in a stack of thin fibrous layers. A fully saturated fibrous layer was brought into contact with a dry layer. During the experiments, they measured the temporal changes of liquid saturation in the top layer. They used the Richards equation as well as a new approach called Reduced Continua Model, RCM in short (see Qin and Hassanizadeh 2014, 2015; Tavangarrad et al. 2018) to simulate the experimental data. They found that Richards equation was not able to reproduce the data, whereas the RCM model could provide a good fit. Similar results were found by Tavangarrad et al. (2019b) in the study of continuous injection of water into a stack of two thin porous layers in the through-plane direction.

In most of these numerical and experimental studies, either imbibition or drainage was investigated, and not consecutive occurrence of both processes in the same domain where capillary hysteresis becomes important. Limited studies have been performed to investigate the hysteretic effect, which is known to exist in unsaturated soil during imbibition

and drainage processes. Moreover, hydraulic properties of thin porous materials may be different in in-plane and through-plane directions due to the special character of thin structures. Studies have shown that the models used for simulating the behavior of thin porous media under unsaturated flow conditions suffer from various shortcomings. For instance, Washburn equation, which has been often used to model liquid imbibition into thin porous media (see, e.g., Giuespie and Chemical 1959; Marmur and Cohen 1997; Testoni et al. 2018), assumes that there is a sharp front between fully saturated and dry domains. This assumption does not hold in many situations. Also, some studies have shown that the Richards equation does not adequately simulate such conditions (e.g., Tavangarrad et al. 2018). Thus, one has to look for alternatives to simulate unsaturated flow in porous media.

In this study, we have performed a series of one-dimensional experiments involving in-plane imbibition and subsequent drainage of water in a thin fibrous layer. The X-ray transmission method was used to measure saturation distributions along the fibrous sample. The experimental data were simulated using two different models: (1) traditional Richards equation and accounting for hysteresis, (2) an extended Richards equation with a so-called dynamic capillarity term, proposed by Hassanizadeh and Gray (1993). The objectives of this study are: (1) to present a set of well-controlled imbibition—drainage experimental data for thin porous media, which may also be used by other researchers, and (2) to investigate the applicability of an alternative approach to simulating unsaturated flow in thin porous media, especially for fast spontaneous imbibition.

2 Methods and Materials

The thin fibrous layer used in this study was a nonwoven material, which was made of regenerated cellulose, commonly used in absorbent tissues. Distilled water was used in all experiments. The porosity of layer and mean radius of fibers were estimated from confocal microscope images of the layer without any compression. Microscope images of the two sides of the thin layer are shown in Fig. 1. The layer thickness was measured without any compression and stick-out fibers were ignored. The in-plane intrinsic permeability was measured through the constant-head method. We measured the layer's imbibition and

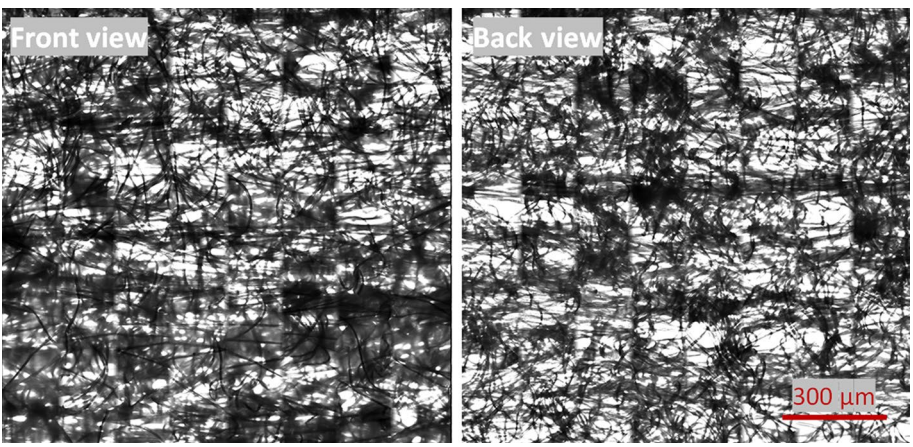

Fig. 1 Microscope images of the two sides of the thin layer

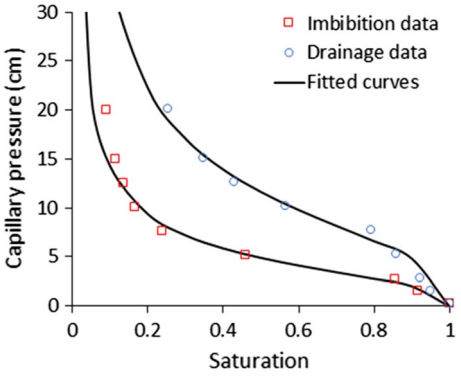

Fig. 2 Measured p^c–S curves for imbibition and drainage obtained via through-plane quasi-static experiments. Parameter values for fitted curves are given in Table 1

Table 1 Properties of the fibrous material used in this study

Parameter	Value
Fiber radius, r (μm)	10 ± 0.5
Fiber density, ρ^f (g/m^2)	40
Layer thickness, D (μm)	705
Porosity, φ (–)	0.96
Intrinsic permeability, k (m^2)	9.4×10^{-10}
Parameter in VG model for imbibition, α (Pa^{-1})	2.6×10^{-3}
Parameter in VG model for imbibition, n (–)	2.74
Parameter in VG model for drainage, α (Pa^{-1})	1.1×10^{-3}
Parameter in VG model for drainage, n (–)	2.74

drainage water retention curves in the through-plane direction using the hanging water column (HWC) method (Dane and Hopmans 2002). The measured data are shown in Fig. 2.

We employed van Genuchten formula (1980) to fit the data:

$$p^c(S) = \frac{1}{\alpha}\left[S_e^{-1/m} - 1\right]^{1/n} \tag{1}$$

with the effective saturation, S_e, defined as:

$$S_e = \frac{S - S_{ir}}{1 - S_{ir}} \tag{2}$$

where $p^c(S)$ denotes the capillary pressure, S and S_{ir} are water saturation and irreducible water saturation, respectively, α and n are fitting parameters, and $m = 1 - 1/n$. The fitted curves are shown in Fig. 2 as solid lines. Values of various parameters for the tissue fibrous material are given in Table 1. Mualem's formula (Mualem 1976) was used for the relative permeability:

$$k^r(S) = S_e^l\left[1 - \left(1 - S_e^{1/m}\right)^m\right]^2 \tag{3}$$

The coefficient l is usually set equal to 0.5 (van Genuchten 1980). The Mualem–van Genuchten model is commonly used for soils to estimate the relative permeability–saturation relationship based on fitting parameters obtained from capillary pressure data.

Due to the lack of relative permeability data, we have employed this model for thin porous media as some other studies have suggested (e.g., Ashari and Vahedi Tafreshi 2009; Tavangarrad et al. 2019a). However, we note that this model should be improved for thin porous media based on experimental measurement of relative permeability specifically designed for thin porous media.

A schematic view of the experimental setup is shown in Fig. 3. A Plexiglas open frame, shown in green, was constructed to support a thin tissue that was placed on thin steel wires. A fully dry fibrous layer, shown in red, with a thickness of 705 μm and dimensions of 3.2 cm (width) × 30.5 cm (length), was placed on the frame. A small clamp was used to fix the end of the layer. For the imbibition experiment, the frame was put horizontally on an X-ray plate. The saturation profiles were measured along the length of the layer every other minute. The measurement domain started at 1 cm from the edge of water reservoir (point A in Fig. 3).

The experiment started by immersing the first 5 cm of the layer into a water reservoir (shown in blue). This ensured full contact with water at all times. The observed saturation was a thickness- and width-averaged value over every 0.5 cm. After about twenty minutes, equilibrium was reached and water imbibition stopped. The drainage experiment was started by rotating the entire system (i.e., the X-ray source and the plate) by 45° so that the sample was in an inclined position (see Fig. 3), and water flowed back from the tissue into the reservoir. The rotation process took one minute. During the entire experiment, the tip of the sample was always kept in the water reservoir in full contact with water, although about 2.8 cm of the sample was hanging in the air during drainage experiments (see Fig. 3). All experiments were conducted in a constant-temperature room at 21 ± 0.5 °C. At least two duplicates were done for all experiments.

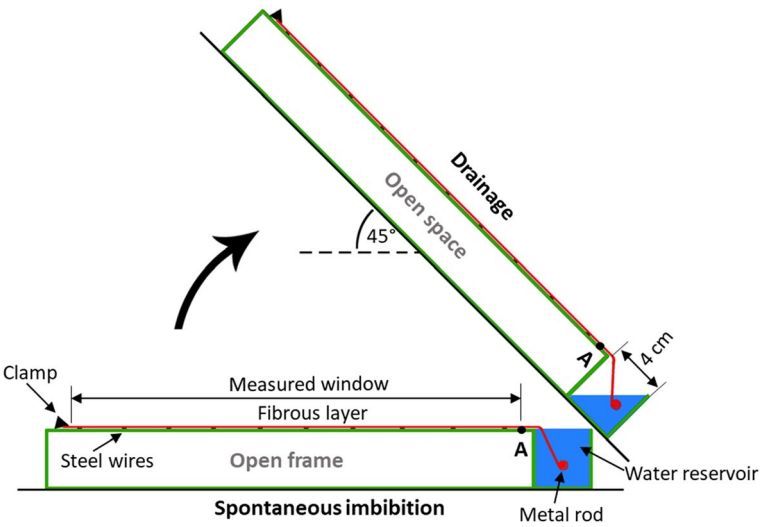

Fig. 3 Schematic view of the experimental setup. Open Plexiglas frame is shown in green and the sample shown in red. Spontaneous imbibition occurred with the setup placed horizontally and the sample tip immersed into the water. Then, the setup was put in an inclined position, which caused drainage to occur

3 Numerical Model

We used the one-dimensional Richards equation to simulate the experiments:

$$\varphi \frac{\partial S}{\partial t} + \frac{\partial}{\partial x}\left[-\frac{k^r(S)k}{\mu}\left(\frac{\partial p^{\mathrm{w}}}{\partial x} + \rho g \sin\beta\right)\right] = 0 \tag{4}$$

where μ is water viscosity, ρ is water density, g is gravity, p^{w} is water (gauge) pressure, t is time, x denotes the distance from the edge of water reservoir, and β is the angle between the flow direction and the horizontal axis. The value of β was equal to 0° during the spontaneous imbibition process, while it was 45° during the drainage process. The swelling effect of fibers was neglected here.

However, studies have shown that the standard Richards equation is not able to capture all flow behaviors in 3-D porous media (e.g., Diamantopoulos and Durner 2012). There have been several different approaches to simulate dynamic effects during multi-phase flow in soils (e.g., Barenblatt 1971; Juanes 2009). Here, the dynamic capillarity effect as formulated by Hassanizadeh and Gray 1990) was included in our simulations. Assuming a linear approximation, it has the following form for an air–water system (Hassanizadeh et al. 2002):

$$-p^{\mathrm{w}} = p^{\mathrm{c}}(S) - \tau \frac{\partial S}{\partial t} \tag{5}$$

where τ is the so-called dynamic capillarity coefficient, which is a material property. Under quasi-static conditions (i.e., $\partial S/\partial t \approx 0$), the difference between water gauge pressure and capillary pressure is negligible. Zhuang et al. (2019) have referred to the combination of Eq. (5) with Richards equation as extended standard model.

During dynamic processes (i.e., $\partial S/\partial t \neq 0$), the difference between water gauge pressure and capillary pressure becomes significant for large flow rates. For sandy soils, it has been found that the pressure difference between the fluid phases is not equal to capillary pressure under dynamic conditions (see, e.g., Smiles et al. 1971; Topp and Peters 1967). Moreover, a number of studies have shown that for a satisfactory simulation of fast unsaturated flow in soil, one has to include the dynamic capillarity effect. For example, DiCarlo (2005). simulated experiments on water infiltration into dry soil and showed that for the modeling of nonmonotonic saturation profiles one has to take into account the dynamic capillarity effect. Similar results have been reported by Zhuang et al. (2019) who also simulated experiments on water infiltration into dry soil. In other experiments, the role of dynamic effect in a proper simulation of water redistribution in soil was shown (Zhuang et al., 2016, 2017a, b). Some experimental and numerical studies have been performed to determine values of τ for soils. Among them, a few studies have shown that τ may be a function of saturation (see, e.g., O'Carroll et al. 2005; Manthey et al. 2008; Bottero et al. 2011; Joekar-Niasar and Majid Hassanizadeh 2011; Diamantopoulos and Durner 2012; Abidoye and Das 2014; Goel et al. 2016; Zhuang et al. 2017a, b; van Duijn et al. 2018). However, form of relationship between τ and saturation is still inconclusive at this moment.

Ideally, one should determine the dynamic capillarity coefficient for thin porous media directly through experiments. Unfortunately, a well-defined experiment would be difficult and complicated. In particular, the measurements of average fluid pressures as a function of time at various points along the thin medium are needed, which would not be straightforward. To the best of our knowledge, there are no direct experimental measurement of the dynamic capillarity coefficient for thin porous media. Tavangarrad

et al. (2018) evaluated τ values based on simulations of through-plane redistribution of water in a stack between two thin porous layers. However, there are no studies of in-plane unsaturated flow in thin porous media using the dynamic capillarity model. Also, the dependence of dynamic capillarity on saturation for thin porous media still have not been studied, up to now. Zhuang et al. (2019) suggested four different functional forms of τ based on results of studies in soils reported in the literature. We performed simulations using those four different functional forms for τ in order to have a general idea about the effect of τ–S relationship for thin porous media. Results are presented in "Appendix 3." We found that the quadratic relationship between τ and saturation provides the best results for simulating current experiments.

We performed three different sets of simulations for both spontaneous imbibition and drainage processes. (1) Simulation I, using Richards equation with measured p^c–S curve (denoted as Curve 1) and corresponding values for α and n as given in Table 1; (2) Simulation II, using Richards equation but with modified p^c–S curves (denoted as Curve 2). Corresponding values for α and n were selected in such a way that the numerical results and the experimental ones were in good agreement. (3) Simulation III, using the Richards equation in combination with the original p^c–S curve (Curve 1) and dynamic capillarity equation. For the latter simulation, various functional forms of the coefficient τ (either as a constant or as a function of saturation) were optimized in order to get best agreement with the observed data.

The full set of equations were solved implicitly using the commercial package COMSOL 5.0 (COMSOL 2014), which is based on the finite element method. The grid size was set to 1×10^{-3} m, and the maximum time step to 0.01 s to achieve mesh-independent solutions. For the simulations of spontaneous imbibition process, the initial saturation along the domain was set equal to a minimum value of 0.01, whereas the value of 0.99 was assigned as the initial saturation for drainage experiments. The boundary saturation at the reservoir side was set to the value of 0.99, and a no-flow condition was imposed at the other end. For drainage simulations, the modeling domain was elongated by 2.8 cm due to include the hanging part of the tissue (see Fig. 3). We also performed supplementary simulations to investigate the effect of evaporation effect on simulation results; that was found to be negligible (details are given in "Appendix 1"). The simulation parameters are summarized in Table 2.

Table 2 Modeling parameters

	Simulation I	Simulation II	Simulation III
Information	With original parameters (curve 1)	With fitted p^c–S curve 2	With dynamic capillarity equation and curve 1
Maximum time step	0.01 s		
Grid size	1 × 10–3 m		
Boundary conditions	Imbibition: x = -0.01 m, S = 0.99; x = 0.245 m, no flow Drainage: x = − 0.01 m, S = 0.99; x = 0.245 m, no flow		
Initial conditions	Imbibition: S = 0.01 Drainage: S = 0.99		

4 Results and Discussion

4.1 Imbibition

Experimental data for imbibition (shown as open circles) and results of three different simulations (shown as solid lines) are given in Fig. 4b–d. The saturation at $x=0$, i.e., the edge of water reservoir, reached the value of 0.90 within 1 min, but then approached the maximum saturation relatively slowly, after about 10 min.

To model the spontaneous imbibition experiments, we focused on three features of the observed data: (1) the temporal variation of measured saturation at $x=1$ cm; (2) the wetted length of the layer at a given time (i.e., the position of saturation front); (3) the curvature of the saturation profiles. As shown in Fig. 4b, the saturation distribution curves obtained from Simulation I are at all times distinctly different from the observations in all three features. The wetted length is at all times significantly larger than measured values (water advances much faster than in experiments). Additional simulations were performed, in which we changed intrinsic permeability value and relative permeability curves. The details and results are given in "Appendix 2". Decreasing the values of relative permeability resulted in a shorter wetted length of the layer and matched measured values at different times. However, the curvature of saturation profiles and the saturation value at $x=1$ cm were still far from measured data. In Simulation II, we tried to fit observed data as closely as possible by adjusting the values of the parameters α and n in the imbibition

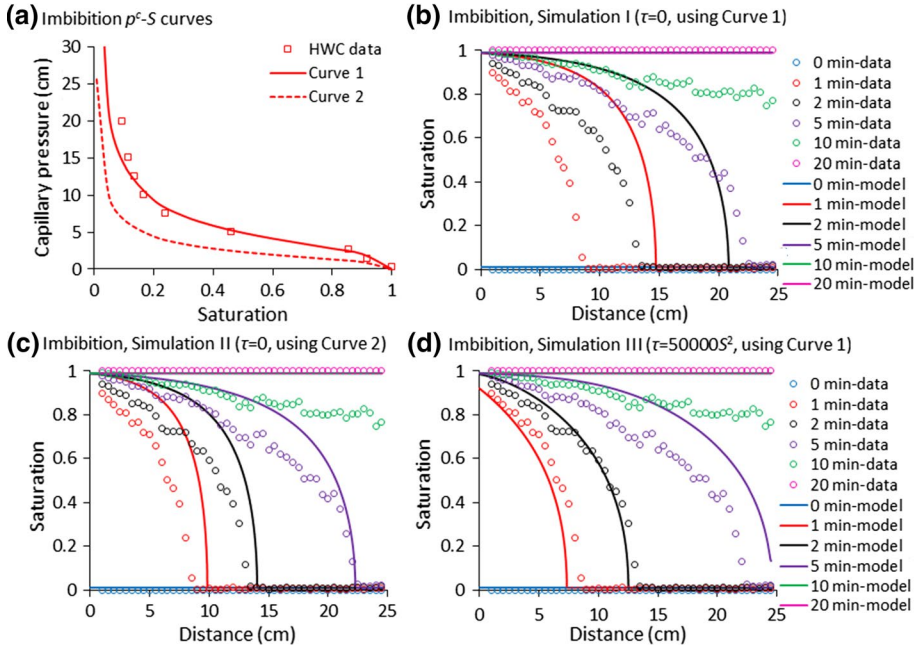

Fig. 4 Experimental and simulation results for the spontaneous imbibition experiment. **a** Measured and fitted p^c–S curves. Observed saturation profiles (open circles), and simulated curves (solid lines) obtained with Simulations I to III (**b**–**d**). The first data point is at $x=1$ cm. Simulation results for the time of 10 min and 20 min overlapped

p^c–S relationship. Hence, we obtained a modified p^c–S curve (shown as Curve 2 in Fig. 4a) by fitting measurements. This also affected the relative permeability curve. This improved the result for the wetted length (see Fig. 4c). However, both the saturation at $x = 1$ cm and the curvature of saturation profiles still deviated from the observations considerably. When we incorporated the effect of dynamic capillarity, we obtained much better agreement with measured data (see Fig. 4d). Although the model with dynamic capillarity equation (Simulation III) fitted the observed data at early times much better, it did not do so at late times, while the standard Richards equation using modified p^c–S curves (Simulation II) gave slightly better agreement with the observed data at some medium times.

Figure 5 shows the changes in average saturation of the whole layer as a function of time. Clearly, the model with dynamic capillarity equation (Simulation III) fitted the observed data at early times perfectly, but it later deviated from the data due to limited dynamics. The main reason for this deviation is most probably the fact that as the tissue gets wet during imbibition, fibers absorb water and swell. This means water leaves the pores, and one should include a sink term to the Richards equation. Unfortunately, we could not model this effect as there was no information on the swelling behavior of fibers.

4.2 Drainage

Experimental and simulation results for the drainage experiments are shown in Fig. 6. As shown in Fig. 6b, the measured saturation along the sample decreased fast within 2 min. The drainage of water slowed down afterward, and equilibrium was reached within 20 min. Simulation I was able to model the observations at 2 min reasonably well, but not at later times. The saturation values obtained from Simulation I at equilibrium all along the domain are significantly higher than the observed data.

Given that equilibrium was almost reached after 20 min, one could derive a set of p^c–S data based on the observed equilibrium saturation distribution at various positions along the sample. At equilibrium, water pressure along the sample follows the hydrostatic pressure distribution. So, at every point, knowing the saturation, we can calculate the water pressure (and thus the capillary pressure). This experimental method can be used to obtain p^c–S data for drainage for the thin porous layer. The resulting p^c–S data are shown as blue dots in Fig. 6a. The fitted curve using van Genuchten model (Curve 2) and the measured through-plane p^c–S curve are shown as dashed and solid lines, respectively. The fitted value

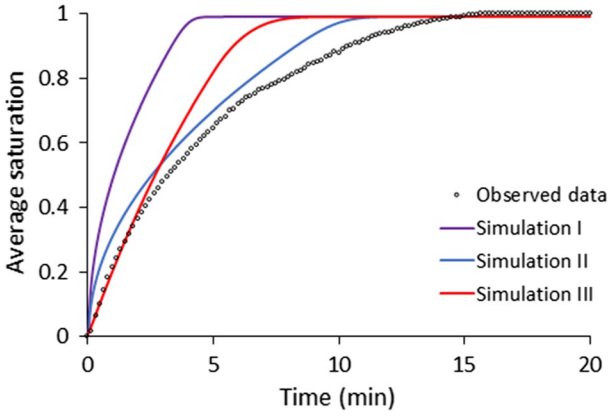

Fig. 5 Change of the average saturation over the entire domain as a function of time during the spontaneous imbibition process

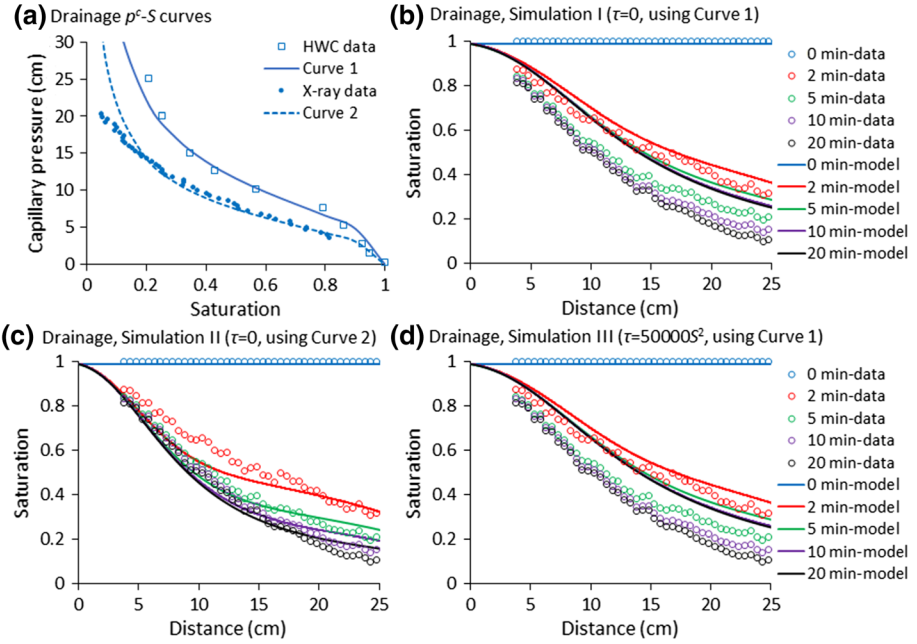

Fig. 6 Experimental and simulation results for the drainage experiment. **a** Measured and fitted p^c–S curves. Observed saturation profiles (open circles), and simulated curves (solid lines) obtained with Simulations I to III (**b**–**d**)

of α for Curve 2 was 1.7×10^{-3} Pa^{-1}, and the fitted n value was the same as the one for Curve 1. By using Curve 2, Simulation II gave a better agreement with the observed data for most times except at $t=2$ min, which we see some deviation. In Simulation III, dynamic capillarity effect was included with the same functional form of τ that was specified for the imbibition process. The results of Simulation III (see Fig. 6d) were almost identical to Simulation II. This indicates that the dynamic capillarity effect is not significant during the drainage as it occurs relatively slowly. This phenomenon has also been found in soils. Temporal changes of saturation are much slower during drainage than imbibition, resulting in negligible dynamic capillarity effect with the same τ values.

One interesting phenomenon regards the different p^c–S curves 1 and 2 shown in Fig. 6a. As explained earlier, Curve 1 is based on drainage experiments in the through-plane direction, while Curve 2 is based on data from in-plane drainage. This implies that p^c–S curves may be different in different directions. However, there are limited experimental studies to investigate in-plane and through-plane p^c–S curves for different thin porous media up to now.

5 Summary and Conclusions

Here, we have presented a set of well-controlled imbibition and subsequent drainage experiments in a thin fibrous layer. The experimental data were simulated using Richards equation either with classical capillary equation or with the dynamic capillarity

term. The results have shown that the standard Richards equation cannot simulate all flow conditions in thin porous media. We have provided an alternative approach by accounting for the dynamic capillarity effect. For this specific fibrous material, we have found:

1. The p^c–S curves which are obtained when water flow is mainly perpendicular to the layer (i.e., through-plane direction) are not necessary applicable for modeling the process when the flow is in the planar direction; the entry pressure in the in-plane direction is lower than that of the through-plane direction. Obviously, our results are not consistent with the fact that both p^c and S are scalar variables. Nevertheless, we think it is important to report the results here.
2. One can simply get the in-plane drainage p^c–S curve using the vertical equilibrium drainage method presented in this study; the p^c–S data can be obtained based on the observed saturation profiles at equilibrium and hydrostatic pressure distribution.
3. Given that spontaneous imbibition is a relatively fast capillary-driven process, one should account for the dynamic capillarity effect in order to model this process. However, the dynamic capillarity effect is not significant during the relatively slow drainage.

Appendix 1: Including Evaporation Effect During Imbibition

The evaporation rate r was measured experimentally. In the experiment, a fully saturated fibrous layer was placed on a stainless-steel porous plate. The temporal changes of weight were recorded using a three-digit precision balance (Kern & Sohn GmbH, Germany). Figure 7 shows the saturation changes in the fibrous layer as a function of time. An evaporation rate of $r = 0.165\ \mathrm{h}^{-1}$ was obtained by fitting the data linearly. We performed a set of simulations including evaporation during spontaneous imbibition process. The governing equations were modified by adding the evaporation term, $-\varphi r$, to the right-hand side of Eq. (4). They are almost identical to the ones shown in Fig. 3a; this indicates that the influence of evaporation is negligible during spontaneous imbibition process here. This is to be expected as the time scale of evaporation was much larger than the one for our experiments (Fig. 8).

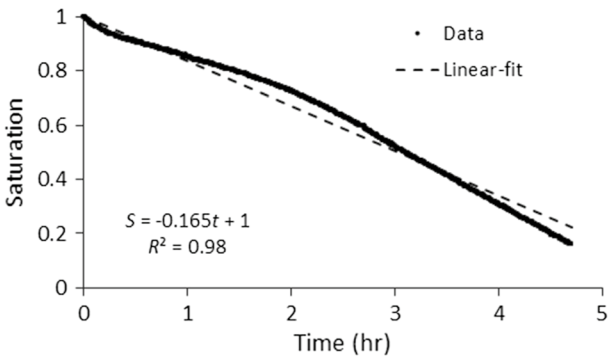

Fig. 7 Saturation changes in the fibrous layer as a function of time during evaporation

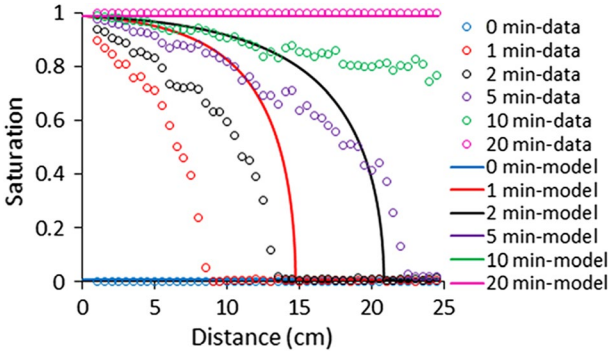

Fig. 8 Observed saturation profiles (open circles) and simulated curves (solid lines) obtained using the classical Richards equation including evaporation effect

Appendix 2: Simulations Obtained by Adjusting Intrinsic and/or Relative Permeabilities

Figure 9a shows the simulation results obtained using the classical Richards equation with the intrinsic permeability value reduced by a factor of 9.2/4.2 = 2.19 compared to the value used in Simulations I–III. In an additional set of simulations, the relative permeability was also reduced by increasing the value of parameter l in Eq. (3) from 0.5 to 1.0. Results are shown in Fig. 9a, b, respectively. It is evident that reducing the intrinsic permeability was capable of decelerating the imbibition process, similarly to decreasing the relative permeability. However, the shape of saturation profiles and saturation value at $x = 1$ cm were unchanged. Clearly, the classical Richards equation was not capable of modeling the spontaneous imbibition process despite adjusting values of intrinsic and/or relative permeabilities.

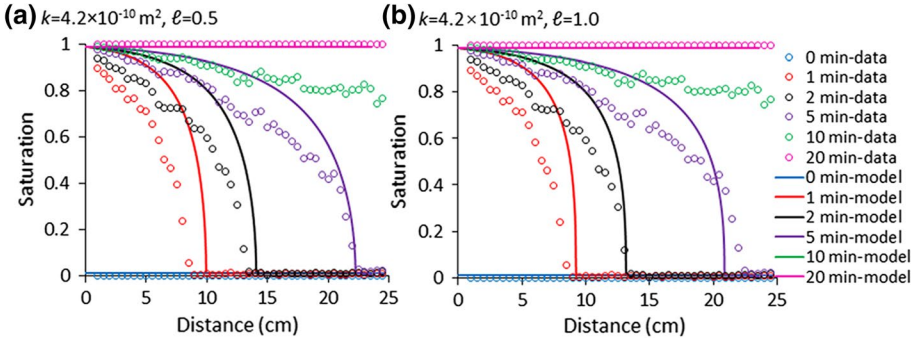

Fig. 9 Observed saturation profiles (open circles) and simulated curves (solid lines) obtained using the classical Richards equation with adjusting intrinsic and/or relative permeabilities

Appendix 3: Simulations Obtained with Different τ–*S* Functions

Based on the studies of dynamic capillarity in soils (Zhuang et al. 2019), we have chosen five typical functional forms for the dynamic capillarity coefficient τ. The functions are shown in Table 3. The constant τ_0 in each function was optimized and may vary in different functional forms. The simulation results using the quadratic power function τ_4 are shown in Fig. 3. The selected simulation results obtained using the remaining four τ–S functions are shown in Fig. 10. Obviously, regardless of τ–S functional forms, including the dynamic capillarity term always improved the agreement with the wetted length of the layer at different times. Specifically, as shown in Fig. 10a, b, for τ_1 and τ_2, the saturation profiles were relatively steep with unchanged saturation at $x = 1$ cm. These simulations curves are not anywhere close to the measured values. The simulations

Table 3 Different expressions for the dynamic capillarity coefficient τ.

Dynamic capillarity function	Expressions
τ_1	τ_0
τ_2	$\tau_0(1-S)$
τ_3	$\tau_0 S$
τ_4	$\tau_0 S^2$
τ_5	$\tau_0 S^3$

The value of constant τ_0 may vary in different functional forms

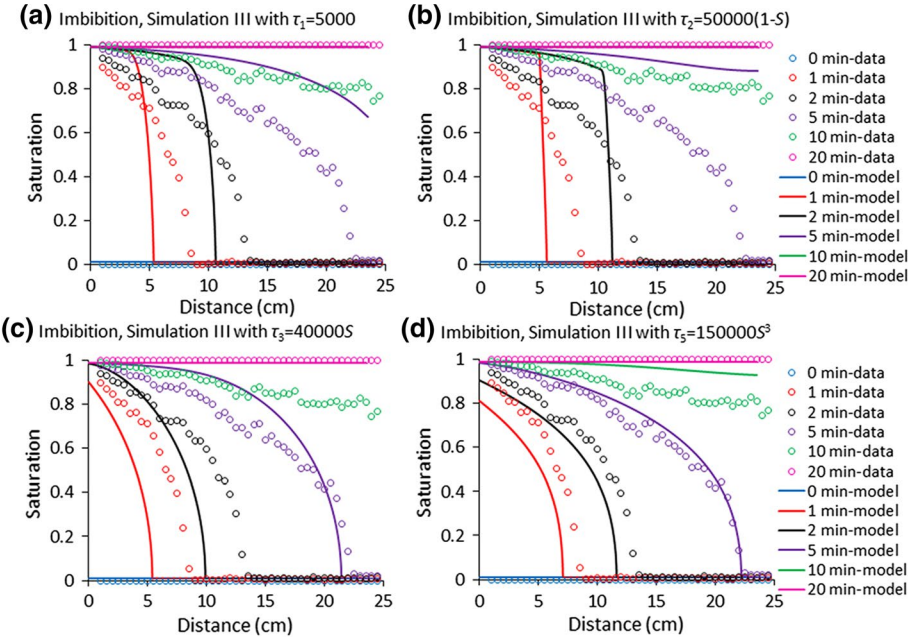

Fig. 10 Observed saturation profiles (open circles) and simulated curves (solid lines) obtained using the extended Richards equation with different τ–S functional forms

using τ_3 (linear) and τ_5 (cubic power) gave a better agreement with the observations (see Fig. 10c, d). However, these results still showed either faster or slower temporal saturation changes at $x=0$. The function τ_4 (quadratic power function), therefore, was chosen as the best form for modeling dynamic capillarity in this work.

Acknowledgements We gratefully acknowledge Ioannis Zarikos and Hamed Aslannejad of Utrecht University for technical support in using the confocal microscope. This work was supported by Kimberly-Clark Corporation and carried out in collaboration with the Darcy Center. The first author received funding from the National Natural Science Foundation of China (Grant No. 42007165). The second author received funding from the European Research Council under the European Union's Seventh Framework Program (FP/2007-2013)/ERC Grant Agreement No. 341225.

Authors' contribution LZ was involved in the methodology, software, validation, and writing–original draft; SMH was involved in the conceptualization, supervision, writing—review and editing, and funding acquisition; DB contributed to the methodology and supervision; CJD contributed to the data analysis and supervision.

Funding This work was supported by Kimberly-Clark Corporation and carried out in collaboration with the Darcy Center. The first author received funding from the National Natural Science Foundation of China (Grant No. 42007165). The second author received funding from the European Research Council under the European Union's Seventh Framework Program (FP/2007–2013)/ERC Grant Agreement No. 341225.

Data Availability The data are available by contacting the corresponding author.

Declarations

Conflict of interest The authors have no conflict of interest to declare.

References

Abidoye, L.K., Das, D.B.: Scale dependent dynamic capillary pressure effect for two-phase flow in porous media. Adv. Water Resour. **74**, 212–230 (2014)

Ashari, A., Vahedi Tafreshi, H.: A two-scale modeling of motion-induced fluid release from thin fibrous porous media. Chem. Eng. Sci. **64**, 2067–2075 (2009)

Ashari, A., Bucher, T.M., Vahedi Tafreshi, H.: A semi-analytical model for simulating fluid transport in multi-layered fibrous sheets made up of solid and porous fibers. Comput. Mater. Sci. **50**, 378–390 (2010)

Ashari, A., Bucher, T.M., Tafreshi, H.V.: Modeling motion-induced fluid release from partially saturated fibrous media onto surfaces with different hydrophilicity. Int. J. Heat Fluid Flow. **32**, 1076–1081 (2011)

Aslannejad, H., Hassanizadeh, S.M., Raoof, A., de Winter, D.A.M., Tomozeiu, N., van Genuchten, M.T.: Characterizing the hydraulic properties of paper coating layer using FIB-SEM tomography and 3D pore-scale modeling. Chem. Eng. Sci. **160**, 275–280 (2017)

Barenblatt, G.I.: Filtration of two nonmixing fluids in a homogeneous porous medium. Fluid Dyn **6**, 857–864 (1971)

Bottero, S., Hassanizadeh, S.M., Kleingeld, P.J., Heimovaara, T.J.: Nonequilibrium capillarity effects in two-phase flow through porous media at different scales. Water Resour. Res. **47**, W10505 (2011)

COMSOL: COMSOL multiphysics 5.0. COMSOL Inc., Burlington, MA (2014)

Dane, J.H., Hopmans, J.W.: Water retention and storage: laboratory. In: Dane, J.H., Topp, G. (eds.), Methods of Soil Analysis: Part 4 Physical Methods, Soil Sci. Soc. of Am., Madison, pp. 675–720 (2002)

Diamantopoulos, E., Durner, W.: Dynamic nonequilibrium of water flow in porous media: a review. Vadose Zone J **11**, vzj2011-0197 (2012)

DiCarlo, D.A.: Modeling observed saturation overshoot with continuum additions to standard unsaturated theory. Adv. Water Resour. **28**, 1021–1027 (2005)

Giuespie, T., Chemical, T.D.: The capillary rise of a liquid in a vertical strip of filter paper. J. Colloid Sci. **1**, 123–130 (1959)

Goel, G., Abidoye, L.K., Chahar, B.R., Das, D.B.: Scale dependency of dynamic relative permeability-satuartion curves in relation with fluid viscosity and dynamic capillary pressure effect. Environ. Fluid Mech. **16**, 945–963 (2016)
Hassanizadeh, S.M., Gray, W.G.: Mechanics and thermodynamics of multiphase flow in porous media including interphase boundaries. Adv. Water Resour. **13**, 169–186 (1990)
Hassanizadeh, S.M., Gray, W.G.: Thermodynamic basis of capillary-pressure in porous-media. Water Resour. Res. **29**, 3389–3405 (1993)
Hassanizadeh, S.M., Celia, M.A., Dahle, H.K.: Dynamic effect in the capillary pressure–saturation relationship and its impacts on unsaturated flow. Vadose Zone J. **1**, 38–57 (2002)
Joekar-Niasar, V., Majid Hassanizadeh, S.: Effect of fluids properties on non-equilibrium capillarity effects: dynamic pore-network modeling. Int. J. Multiph. Flow. **37**, 198–214 (2011)
Juanes, R.: Nonequilibrium effects in models of three-phase flow in porous media. Adv. Water Resour. **31**, 661–673 (2009)
Landeryou, M., Eames, I., Cottenden, A.: Infiltration into inclined fibrous sheets. J. Fluid Mech. **529**, 173–193 (2005)
Manthey, S., Hassanizadeh, S.M., Helmig, R., Hilfer, R.: Dimensional analysis of two-phase flow including a rate-dependent capillary pressure–saturation relationship. Adv. Water Resour. **31**, 1137–1150 (2008)
Marmur, A., Cohen, R.D.: Characterization of porous media by the kinetics of liquid penetration: the vertical capillaries model. J. Colloid Interface Sci. **189**, 299–304 (1997)
Melciu, I.C., Pascovici, M.D.: Imbibition of liquids in fibrous porous media. In: IOP Conference Series: Materials Science and Engineering, vol. 147, p. 012041 (2016)
Mualem, Y.: A new model for predicting the hydraulic conductivity of unsaturated porous media. Water Resour. Res. **12**, 513–522 (1976)
O'Carroll, D.M., Phelan, T.J., Abriola, L.M.: Exploring dynamic effects in capillary pressure in multistep outflow experiments. Water Resour. Res. **41**, 1–14 (2005)
Prat, M., Agaësse, T.: Thin porous media. In: Kambiz, V. (ed.), Handbook of Porous Media, Taylor&Francis, London, p. 959 (2015)
Qin, C.Z., Hassanizadeh, S.M.: Multiphase flow through multilayers of thin porous media: general balance equations and constitutive relationships for a solid–gas–liquid three-phase system. Int. J. Heat Mass Transf. **70**, 693–708 (2014)
Qin, C.Z., Hassanizadeh, S.M.: A new approach to modelling water flooding in a polymer electrolyte fuel cell. Int. J. Hydrogen Energy. **40**, 3348–3358 (2015)
Reza, M., Pillai, K.M.: Darcy's law-based model for wicking in paper-like swelling porous media. AIChE J. **56**, 2257–2267 (2010)
Richards, L.A.: Capillary conduction of liquids through porous mediums. Physics **1**, 318–333 (1931)
Smiles, D.E., Vachaud, G., Vauclin, M.: A test of the uniqueness of the soil moisture characteristic during transient, nonhysteretic flow of water in a rigid soil1. Soil Sci. Soc. Am. J. **35**, 534–539 (1971)
Tavangarrad, A.H., Mohebbi, B., Hassanizadeh, S.M., Rosati, R., Claussen, J., Blümich, B.: Continuum-scale modeling of liquid redistribution in a stack of thin hydrophilic fibrous layers. Transp. Porous Media. **122**, 203–219 (2018)
Tavangarrad, A.H., Hassanizadeh, S.M., Rosati, R., Digirolamo, L., van Genuchten, M.T.: Capillary pressure–saturation curves of thin hydrophilic fibrous layers: effects of overburden pressure, number of layers, and multiple imbibition–drainage cycles. Text. Res. J. **89**, 4906–4915 (2019a)
Tavangarrad, A.H., Mohebbi, B., Qin, C., Hassanizadeh, S.M., Rosati, R., Claussen, J., Blümich, B.: Continuum-scale modeling of water infiltration into a stack of two thin fibrous layers and their inter-layer space. Chem. Eng. Sci. **207**, 769–779 (2019b)
Testoni, G.A., Kim, S., Pisupati, A., Park, C.H.: Modeling of the capillary wicking of flax fibers by considering the effects of fiber swelling and liquid absorption. J. Colloid Interface Sci. **525**, 166–176 (2018)
Topp, G., Peters, A.: Comparison of water content-pressure head data obtained by equilibrium, steady-state, and unsteady-state methods1. Soil Sci. Soc. Am. J. **31**, 312–314 (1967)
van Genuchten, M.T.: A closed-form equation for predicting the hydraulic conductivity of unsaturated soils. Soil Sci. Soc. Am. J. **44**, 892–898 (1980)
van Duijn, C.J., Mitra, K., Pop, I.S.: Travelling wave solutions for the Richards equation incorporating non-equilibrium effects in the capillarity pressure. Nonlinear Anal. Real World Appl. **41**, 232–268 (2018)
Washburn, E.W.: The dynamics of capillary flow. Phys. Rev. **XVII**, 273–283 (1921)
Zhuang, L., Hassanizadeh, S.M., van Genuchten, MTh., Leijnse, A., Raoof, A., Qin, C.: Modelling of horizontal water redistribution in an unsaturated soil. Vadose Zone J. **15**, 3 (2016)
Zhuang, L., Hassanizadeh, S.M., Kleingeld, P., van Genuchten, M.: Revisiting the horizontal redistribution of water in soils; experiments and numerical modeling. Water Resour. Res. **53**, 7576–7589 (2017a)

Zhuang, L., Hassanizadeh, S.M., Qin, C.-Z., de Waal, A.: Experimental investigation of hysteretic dynamic capillarity effect in unsaturated flow. Water Resour. Res. **53**, 9078–9088 (2017b)
Zhuang, L., van Duijn, C.J., Hassanizadeh, S.M.: The effect of dynamic capillarity in modeling saturation overshoot during infiltration. Vadose Zone J. **18**, 180133 (2019)